NOLTR 61-67

THE CHARACTERISTICS OF ELECTRIC SPARK DISCHARGES IN MIXTURES OF HIGH-EXPLOSIVE AND ALUMINUM POWDERS

25 AUGUST 1961

NOL
UNITED STATES NAVAL ORDNANCE LABORATORY, WHITE OAK, MARYLAND

THE CHARACTERISTICS OF ELECTRIC SPARK DISCHARGES IN MIXTURES OF HIGH-EXPLOSIVE AND ALUMINUM POWDERS

Prepared by:

T. P. Liddiard, Jr.

Approved by: Aaron D. Solem
Chief, Explosion Dynamics Division

ABSTRACT: A method is described for obtaining the average resistance of a spark discharging through a granular conductive mix (RDX/aluminum - 97/3, or sugar/aluminum - 97/3) in a non-oscillating discharge system. The spark resistance is a linear function of the spark gap width for a given electrode arrangement. The resistance is relatively independent of the density of the mix over the range 0.7 to 0.9 g/cm^3. For the discharge of a 1-mfd capacitor charged to 5.0 kv with total circuit resistance of 0.9 ohm (spark resistance of 0.18 ohm -- gap width 0.25 mm for 30° electrode tips) peak current is about 2200 amps, and peak power is 0.89 megawatts reached in 2.0 microsec. The energy dissipated by the spark in this interval is 7.9% of that stored by the capacitor.

PUBLISHED SEPTEMBER 1961

EXPLOSIONS RESEARCH DEPARTMENT
U. S. NAVAL ORDNANCE LABORATORY
WHITE OAK, MARYLAND

This work was undertaken as part of the Naval Ordnance Laboratory's general program devoted to studying explosives, initiation of explosives and explosive compositions, and the growth from initiation to detonation in such materials. This work was carried out under Task NOL-260, Project LACE.

This work should be of interest to investigators of electric discharge phenomena as well as investigators in the field of explosives research.

The author wishes to acknowledge the able assistance of James Schneider in carrying out the experiments and of James E. Counihan in preparing electronic components.

W. D. COLEMAN
Captain, USN
Commander

C. J. Aronson

C. J. ARONSON
By direction

CONTENTS

TABLES

TABLES (Cont'd.)

FIGURES

THE CHARACTERISTICS OF ELECTRIC SPARK DISCHARGES IN MIXTURES OF HIGH-EXPLOSIVE AND ALUMINUM POWDERS

1. INTRODUCTION AND BACKGROUND

In the course of investigations on electric-spark initiation of high-explosive "conductive mixes" at this Laboratory, a detailed study was made of the electrical characteristics of the discharge circuit and of the initiating spark occurring in the mixture. The more detailed results of this phase of the study are considered important enough, in themselves, to be given here separately from the overall results, the latter being mostly concerned with the initiation and detonation of the explosive (1,2). The objective of the portion of the investigation reported here was to determine the resistance of the spark occurring in an explosive conductive mix and, hence, the power and energy delivered to the spark. In order to do this adequately, the behavior of the complete discharge system was studied, with and without the spark load.

The typical explosive conductive mix used in the tests was 97% RDX and 3% fine-flake aluminum by weight, commonly designated RDX/aluminum (97/3). The RDX had a fairly wide range of particle sizes, the mean particle size having a diameter on the order of 20 to 25 microns. The aluminum, Alcoa 422, had an average diameter of about 10 microns and a thickness of 0.3 micron. It is estimated that the Alcoa 422 was 97% metallic aluminum and 3% aluminum oxide, based on an oxide coating of 50A (3). The name "conductive mix" is, perhaps, misleading, since the resistance between electrode tips may exceed 10^9 ohms before a high voltage is applied. However, the presence of a few percent of aluminum, in effect, reduces the "dielectric strength" of the explosive mixture to well below that of the pure explosive.

This report covers the experimental measurement and determination of the values of the circuit parameters used in the study; a determination of the average resistance (to maximum current) of the spark for a typical explosive conductive mix and for a simulated mix of sugar and aluminum; an evaluation of voltage, power, and energy for the three parameters (L, C, and R) of the complete firing system; and an evaluation of the instantaneous power and accumulated energy expended in the spark region alone. An appendix is included giving an analysis of a series LCR discharge circuit.

2. THE DISCHARGE CIRCUIT

The response of a simple LCR series discharge circuit is well known. The addition of a spark (either as a switch or a load) and a length of coaxial cable, such as used in the conductive mix experiments, however, complicates the behavior of such a circuit. This type of circuit with the spark and cable is shown in Figure 1. In functioning, the 1.0-mfd capacitor is initially charged to some high voltage (5.00 kv throughout most of this study). Discharge is then produced by closing the hydrogen thyratron switch. Before spark breakdown occurs in the conductive mix at the end of the cable an infinite impedance effectively is presented to the electrical pulse. This condition causes voltage doubling at that end of the cable and reflections occur until the spark is established. The spark resistance, once the spark is established, goes through an intermediate phase, exhibiting a resistance of, perhaps, several hundred ohms before it drops to a very low value (4). In the low-potential-arc phase more reflections occur because of the low impedance relative to the impedance of the cable. The picture is further complicated by the presence of high-frequency hash that is characteristic of sparks.

Although the events occurring in less than 0.1 microsec may be quite important in initiating an explosive, it was found, during the course of the conductive mix study, that the spark column must grow (acting as a piston against the explosive) for a much longer time if the initiation is to produce a detonation (1). (Initiation can be produced without detonation necessarily occurring (5).) Because of the predominance of the growing spark as the means of producing detonation, the early occurring events have been essentially disregarded in this analysis.

3. THE CIRCUIT ELEMENTS AND EXPERIMENTAL DETERMINATION OF CIRCUIT PARAMETERS

3.1 The Energy Source

For much of the conductive mix study a 1.0-mfd capacitor (General Electric Type CP70EIEN105K) was used to supply the spark energy. A periodic check was maintained on the capacitor. If the capacitance fell appreciably below the original measured value, the capacitor was replaced. The measurements of capacity were made with an impedance bridge (General Radio Type 650A). A standard mica, 1.0-mfd capacitor (± 0.25%) was used as a check. It was suspected that the capacitance of the energy-

supplying capacitor might deviate appreciably, during a high-current discharge, from the value measured on the bridge. However, oscilloscope measurements of the half-period ($\tau/2$), maximum current (i_{max}), and the time to reach maximum current ($t_{i\ max}$) indicated that the capacitance of the capacitor during discharge remained unchanged at the value given by the impedance bridge measurements.

3.2 The Coaxial Cable

The 7.6-meter long coaxial cable, connecting the pulse generator with the explosive charge, was type C, having a nominal characteristic impedance of 30 ohms. Measured values of the resistance, capacitance, and inductance of the cable were 0.218 ohms, 0.001153 mfd, and 1.68 microh, respectively. The calculation of the impedance, $Z = \sqrt{L/C}$, thus gives a value of 38.2 ohms. (This high value may have been due to manufacturing deviations from nominal values.)

The resistance and inductance of the cable at frequencies near and above that of the natural discharge frequency (0.1 Mc) of the circuit, including the 7.6-meter cable, were obtained with a radio frequency bridge (General Radio Type 916-A). It is likely that the skin effect of the cable becomes important only at frequencies above 0.33 Mc, as indicated in Table I and Figure 2. This would be true if the straight-line relation of R vs. $\sqrt{f}$ held down to its intersection with the D.C. resistance line (0.22 ohm) extending parallel with the abscissa. The inductance (L), also Table I and Figure 2, rose at both the high and low ends of the frequency scale. The deviation at the higher frequencies can be explained by the approach toward infinite impedance at the anti-resonant frequency of 7.2 Mc. This corresponds to a wave-length of four times the length of the shorted-out cable (6). The rise in inductance at the low end was due, at least in part, to poor readability of the dial scale in this region. The inductance value was reasonably linear between 0.75 and 2.50 Mc, being 1.68 microh near the minimum portion of the curve.

3.3 The Current Measuring Resistor

Current pulses from the capacitor, discharging into the coaxial cable which was shorted out at the far end, were obtained for 7.6 meters and 15.2 meters of cable. (Although 7.6 meters was used throughout most of the conductive mix study, the longer cable also was used to enable a check to be made on the circuit parameters. The additional length of cable gave a known increase in inductance and resistance to the circuit.) The current-measuring resistor was of a folded-ribbon

type (7) which effectively cancelled the inductance, Figure 1. The resistance values of several such resistors (manganin ribbon) used in this study were between 0.010 and 0.020 ohm. The skin effect at the natural discharge frequency, neglecting reflections, would be negligible. For any one resistor, the current values were reproducible to ± 3% over an interval of several months. A typical current pulse, with the far end of the cable shorted out, is shown in Figure 3A. The time scale is about 1.0 microsec/division and the maximum current about 2400 amp. (A Tektronix 517 oscilloscope was used with No. 44 Polaroid film in a DuMont Type 302 oscilloscope camera to obtain these records.)

3.4 Simultaneous Voltage-Current Measurements

The voltage-current oscillograms, typical examples shown in Figures 3B and 3C, were obtained with a dual-trace oscilloscope (Tektronix 551). The current signal was obtained from the current-reading resistor. The voltage signal was obtained by a low-inductance voltage divider located at the input to the energy-carrying coaxial cable, i.e. across X-X, Figure 1. The hash at the beginning of the traces was due largely to the hydrogen thyratron switch and to reflections in the main coaxial cable. The shape of the voltage curves and the time to reach zero voltage check very well with the calculated (voltage vs. time) curve for the capacitance, Figure 7, thus giving added validity to the measurements. The current and voltage traces of Figure 3B (7.6-meter cable) were made at initial capacitor voltages of 2, 3, 4 and 5 kv. The current and voltage traces of Figure 3C were made using 7.6- and 15.2-meter cables with initial capacitor voltages of 5 kv. A 5-Mc crystal-controlled oscillator was used to check the sweep speed of the oscilloscope. (Each horizontal division on the prints is about 1.0 microsec.)

3.5 Total Circuit Resistance and Inductance

Average values of the current (i), half-period ($\tau/2$), and time to reach peak current ($t_{i\ max}$), starting with the capacitor charged to 5.0 kv, were obtained from traces as shown in Figure 3C, for both 7.6- and 15.2-meter cables. These are given in Table II. Using these values, a determination of the total circuit resistance and inductance was made. To find these values, the equations

$$L = \frac{1}{2a} R \qquad (1)$$

and

$$L = \frac{\frac{1}{C} + \sqrt{\frac{1}{C^2} - \beta^2 R^2}}{2\beta^2} \qquad (2)$$

(derived from equations (A5) and (A9) in the appendix) were solved simultaneously for L in terms of R. The value of the constant "a" was found from equation (A15). The capacitance of the circuit was experimentally determined to be 0.985 mfd. (The initial capacitor voltage was, of course, positive, the pulse voltage therefore being negative.)

For the 7.6-meter coaxial cable: the half-period was 4.80 microsec, giving a frequency of 0.10420 Mc; the constants, a and β, were 0.16145 and 0.65470, respectively; and the time to reach peak current was 2.03 microsec.

For the 15.2-meter cable: the half-period was 6.24 microsec, the frequency was 0.08000 Mc; the constants a and β, were 0.12503 and 0.50266, respectively; and the time to reach peak current was 2.64 microsec.

(Although the fifth decimal place was preserved throughout the calculations, the measured values may have been off by several percent in some of the parameters.)

A graphical solution for L and R is shown in Figure 4, using the above values. The values of L and R which satisfy the equations, using 7.6- and 15.2-meter cables, are 2.232 microh, 0.721 ohm and 3.78 microh, 0.945 ohm, respectively. The value of 0.224 ohm obtained for ΔR is in good agreement with the D.C. resistance measurement for 7.6 meters of type C coaxial cable, Table I and Figure 2. The value of 1.55 microh for ΔL is about 8% lower than 1.68 microh obtained by the impedance-bridge method, also Table I and Figure 2. This is considered to be a satisfactory check, considering the difficulties involved in making the measurements. An extrapolation to zero cable length in Figure 4 shows that the inductance and resistance of the pulse generator alone were 0.70 microh and 0.50 ohm, respectively.

4. MEASUREMENT OF SPARK RESISTANCE

4.1 The Approach to Obtaining Spark Resistance

If the simultaneous current through and voltage across a spark are measured, the instantaneous power developed in the spark is easily determined. This is simply the product, at a

given time, of the voltage and current. However, it is extremely difficult to get reliable oscilloscope measurements of the component of voltage developed across the spark gap that is the result of the spark resistance alone. The difficulty is due to several things.

First, the inductance existing in the spark can generate a large inductive voltage component. (This inductance includes the portion of the electrodes which are between the contact points of the leads of the measuring cable.) This signal swamps the desired resistive-voltage component.

Second, hash from the hydrogen thyratron switch obscures early detail.

Third, a voltage divider used across the spark is subject to extraneous radiation pick-up because of its relatively high impedance as compared to that of the current-measuring resistor.

With care it may be possible to subtract out the inductive voltage component, provided no other distortions exist. However, a way of obtaining spark resistances, which does not have these difficulties, was used in this study and is presented here.

Before describing the method actually used, it is to be noted that the spark energy could be measured if the circuit were permitted to oscillate. A fairly good indication of the total circuit resistance could be obtained, in an oscillatory (LCR) discharge, from the decrement of the sine-wave variation of the current. Naturally, this method cannot be used if a uni-directional switch, such as a hydrogen thyratron, is used in the circuit. Also, the method cannot be used when the circuit is nearly critically damped or if it is over-damped.

4.2 Spark Resistance with a Switch in the Circuit

When a hydrogen thyratron is used, as in the conductive mix experiments, the spark resistance can be obtained by measuring the peak current with the spark gap in operation. This is compared with the peak current measured with the gap shorted out. Then the change in peak current essentially is due to the resistance of the spark. (A change may also take place in the switch resistance, but this is assumed to be quite small.) The circuit is kept as nearly the same as possible, with and without the spark. Small differences in the short leads at the end of the cable, that occur from one test to the next, do not change the overall inductance appreciably. This

is because most of the circuit inductance is contributed by the coaxial cable leading to the spark gap.

The values of the circuit parameters used to determine the spark resistance were those given in the preceding section, i.e. C = 0.985 mfd, L = 2.232 microh, and E = 5.00 kv. In Table III are shown, as functions of the circuit resistance (R), the frequency of oscillation (f), the peak current (i_{max}), and the time to reach that peak ($t_{i\ max}$). The latter, in microseconds, was calculated from (A15) of the appendix. The total circuit resistance is in ohms, and the capacitance in microfarads. The frequency, if the circuit were allowed to oscillate, i.e. without the uni-directional switch, is in megacycles per second. (Proof of the oscillatory condition is shown in Figure 3D. This shows a current trace which is oscillating at 0.104 Mc. Here the current through the hydrogen thyratron reversed due to an abnormal arc-over. The conditions otherwise were as those used in making the trace of Figure 3A.) The peak current was calculated for various values of circuit resistance from Equation (A7) of the appendix, i.e.

$$i_{max} = \frac{E}{\beta L} \exp\left\{ - a t_{i\ max}\right\} \cdot \sin \beta\, t_{i\ max} \qquad (3)$$

or

$$i_{max} = \frac{E\sqrt{LC}}{L} \exp\left\{ - a t_{i\ max}\right\} . \qquad (4)$$

[Equations (3) and (4) can be shown to be equivalent from Equation (A8), appendix, since at $t_{i\ max}$, $di/dt = 0$ and $\cos \beta\, t_{i\ max} = a \sin \beta\, t_{i\ max}$. •It follows that

$$\sin \beta t_{i\ max} = \frac{\beta}{a} \cos \beta t_{i\ max} = \frac{\beta}{a} \left(\frac{a}{\sqrt{a^2 + \beta^2}} \right) =$$

$$\frac{\beta}{\sqrt{\frac{R^2}{4L^2} + \left(\frac{1}{LC} - \frac{R^2}{4L^2} \right)}} = \beta\sqrt{LC} \, .]$$

Figure 5 shows the maximum current as a function of the total resistance.

With no spark in the circuit, i.e. with the end of the cable (spark end) shorted out, the peak current for a circuit with the above values for C, E, and L was calculated to be

2392.9 amp, R being 0.721 ohm. These values are indicated by the dashed lines in Figure 5 and are used as reference coordinates. The actual current measurements for this shorted-out condition over several months gave values of 2200 to 2500 amp, indicating small drifts in the values of the circuit parameters. For each conductive mix test, one or two calibration pulses also were recorded, i.e. current pulses with the spark end of the cable shorted out. The ratio of the current through the conductive mix spark to the peak current of the calibration pulse was used to get the total circuit resistance. This ratio was multiplied by 2392.9 amp, the calculated (no spark) value for the idealized circuit. This adjusted value of peak current was used to find the total resistance of the circuit (with spark) from Figure 5. (This process thus minimizes the error that occurs due to parameter drift of the circuit components.) Having obtained the total circuit resistance with the spark, subtraction of the resistance of the circuit without the spark, i.e. 0.721 ohm, gave the average resistance of the spark itself.

4.3 The Effect of Electrode Configuration

Current pulses were measured for a number of conditions of the electrodes and the conductive mix. To speed the work, eliminating the need of a firing chamber, a simulated mix made up of powdered-sugar/aluminum (97/3) was used in most of these experiments. The experimental cartridge was a thin disc of mix held in a Plexiglas container, Figure 1. The range of electrode-gap widths used was from 0.1 to 3.2 mm. Most of the electrodes were of copper produced by a printed circuit technique. The thickness of the copper was 0.04 mm and the width was 1.6 mm with a 30° taper, angle α in Figure 1. A few shots were made with aluminum electrodes, 0.05 mm thick and 3.2 mm wide with the same 30° taper. Two densities of the sugar/aluminum mixture were used, one about 0.7 g/cm^3 and the other 0.9 g/cm^3. In some of the experiments with copper electrodes the space between the electrode tips was painted with a dispersion of fine flake aluminum in ethylene chloride, Table IVB. This was found to aid electrical breakdown, especially with gap widths greater than about 1.3 mm, without appreciably altering the spark resistance.

The resistance of the spark (R_s), measured in sugar/aluminum under these various conditions, is shown in Tables IV A, B, and C and plotted as a function of gap width (S) in Figure 6. Note that most of the points, using 30° electrodes, fall close to the straight line,

$$R_s = 0.154 + 0.116\ S, \qquad (5)$$

irrespective of the electrode material or the loading density. The resistance is in ohms and the gap width in millimeters. Measurements with RDX/aluminum (97/3), Tables IVD and IVE, also fell close to the line, Equation (5), except for one low point and one high point. The loading densities used in these experiments were 0.8, 0.9, and 1.2 g/cm^3.

Further experiments were made to clear up the question of why the line in the graph has an intercept with the abscissa at minus 1.3 mm. Two explanations were considered. First, the metal tips of the electrodes erode rapidly, causing an effective widening of the spark gap. Second, there is an appreciable contact resistance between the plasma and the surfaces of the very hot metal electrodes. Copper electrodes with a 120° taper were tried with sugar/aluminum (97/3) at densities of 0.7 and 0.9 g/cm3. These blunter electrodes should not widen with erosion as much as the sharper tips. Therefore, any given initial spark-gap width should give a lower average spark resistance than is produced by the sharper tips. This was confirmed as seen by the results in Table IVF and in the lower line in Figure 6,

$$R_s = 0.058 + 0.122\ S \quad . \qquad (6)$$

The intercept with the abscissa is about minus 0.5 mm as compared to the intercept of 1.3 mm for the 30° electrodes.

Framing camera pictures (Beckman-Whitley Model 189) were made of the erosion of 0.05-mm thick aluminum electrodes in a sugar/aluminum mixture. The electrodes were with a 30° taper and spaced 0.8 mm apart. The rate of gap erosion was fairly linear, 0.28 mm/microsec, up to the limit of observation, 3.5 microsec. The predicted erosion, based on the graph, is 1.3 mm in about 2.0 microsec ($t_{1\ max}$). The observed erosion in the same interval is about one-half this value (0.56 mm). It is likely, then, that both a rapid erosion of the electrode tips and an appreciable contact resistance of the plasma with the electrodes are responsible for the negative abscissa intercept.

4.4 Spark Resistances in Different Media

A spark occurring in air was found to have about one-fourth the resistance of a spark occurring in sugar/aluminum (97/3) at 0.7 g/cm^3. In both cases the aluminum (30°) electrodes were backed by glass slides, forming 3.0-mm gaps. The establishment of the spark in air was aided by dusting a very small amount of conductive mix onto the gap region. The resistance of the spark was determined to be 0.14 ohm in air and 0.59 ohm in the mix.

The resistance of a spark in pure RDX was not obtained. (Measurement could not be easily obtained, since the spark, if established at all, would not be reproducible in time.) However, there is no apparent reason for believing the resistance of the spark in RDX to be appreciably different from that of the spark in the conductive mix, RDX/aluminum (97/3).

5. CALCULATION OF POWER AND ENERGY DELIVERED TO THE SPARK

Once the evaluation of the spark resistance is completed, it is possible to calculate the instantaneous power going into the spark and the energy absorbed or dissipated by the spark. Many of the constants used in these calculations have been evaluated in previous sections. Already given were:

$C = 0.985$ mfd

$E = 5.00$ kv

$L = 2.232$ microh

$R = 0.721$ ohm (without spark).

A total circuit resistance of 0.900 ohm, with spark, was chosen for the following calculations. This gives 0.179 ohm for the spark resistance, a reasonable value for a 0.25- or a 0.50-mm gap, as indicated in Figure 6. In Table III values corresponding to the case where $R = 0.900$ ohm are underlined. These are: $f = 0.10243$ Mc, $t_{i\ max} = 1.9690$ microsec, and $i_{max} = 2233.0$ amp. The constants, a and β, were 0.20161 and 0.64359, respectively.

An evaluation of the current (i) as a function of time for this particular case was made using Equation (A7) of the appendix. The current values are shown in Table V. Also given are the voltages developed across the total circuit resistance (e_R), the lumped inductance (e_L), and the capacitance (e_C) as functions of time. Equations (A19), (A20), and (A21) were used in these latter determinations, the results being shown graphically in Figure 7.

The instantaneous power distribution (Table VI and Figure 8) for R, L, and C was calculated from Equations (A24), (A25), and (A26), Appendix A. The total power developed by the three components at any instant is equal to zero, Equations (A22) and (A23). The energies stored or dissipated by each of the three components were obtained from Equations (A28), (A29) and (A30). The total energy, W, available from the capacitor is 12.31

joules. The energy dissipated in the resistance includes that dissipated in the spark. These results are given in Table VII and in Figure 9.

The fraction of the power and energy going into the total circuit resistance that is due to the spark is 0.179/0.900 or about 20%. The power developed in the spark and the energy absorbed by the spark were determined as functions of time, Table VIII and Figure 10. It is seen that maximum power is reached in about 2.0 microsec, the same time that maximum current is reached. The energy is absorbed rather slowly at the spark, only about 1.5% of the total available energy being absorbed in 1.0 microsec.

6. SUMMARY

A method of obtaining the average resistance of a spark discharging through a granular conductive mix in a non-oscillating discharge system has been described. The spark resistance is shown to be a linear function of the spark-gap width for a given electrode arrangement. This resistance is relatively independent of the density of the conductive mix over the range 0.7 to 0.9 g/cm^3, and of the electrode material, whether aluminum or copper. Sugar/aluminum (97/3) or RDX/aluminum (97/3) mixtures gave comparable results. The power delivered to, and the energy absorbed by, the spark was determined for a typical conductive mix. In the case of discharge of a 1.0-mfd capacitor charged to 5.00 kv, when the spark resistance is taken to be 0.179 ohm or about 20% of the total circuit resistance, the peak power in the spark (for the conditions used) is about 0.89 megawatt, reached in 2.0 microsec. The energy is dissipated by the spark rather slowly, about 1.5% of the 12.3 joules available in 1.0 microsec and only 7.9% in 2.0 microsec.

7. REFERENCES

(1) T. P. Liddiard, Jr., and B. E. Drimmer, "The Electric-Spark Initiation of Mixtures of High Explosives and Powdered Electrical Conductors", ONR Symposium Report ACR-52, Vol. 3, Third Symposium on Detonation, Princeton Univ., Sept. 26-28, 1960; and Proceedings of Electric Initiator Symposium, The Franklin Inst., Philadelphia, Nov. 29-30, 1960. (Conf.)

(2) Howard Leopold, "Investigation of High Explosive Conductive Powder Mixes for Use in Insensitive Electric Initiators", NavWeps Report 6902, 15 Oct 1960 (Conf.)

(3) J. M. Rosen, of this Laboratory (private communication).

(4) J. W. Beams, A. R. Kuhlthau, A. C. Lapsley, J. H. McQueen, L. B. Snoddy, and W. D. Whitehead, Jr., "Spark Light Source of Short Duration", J. Opt. Soc. Am. 37, 868 (1947).

(5) F. P. Bowden and A. D. Yoffe, "The Initiation and Growth of Explosions in Liquids and Solids" (Cambridge Univ. Press, 1952).

(6) R. I. Sarbacher and W. A. Edson, "Hyper and Ultrahigh Frequency Engineering", (John Wiley and Sons, 1943) pp. 334-345.

(7) E. A. Martin, "The Underwater Spark: An example of Gaseous Conduction at about 10,000 Atmospheres", Engineering Research Institute, Univ. of Mich., Ann Arbor, July 1956.

(8) E. B. Kurtz and G. F. Corcoran, "Introduction to Electric Transients" (John Wiley and Sons, 1935).

(9) G. P. Harnwell, "Principles of Electricity and Electromagnetism" (McGraw-Hill, 1938) pp. 421-425.

APPENDIX A

ANALYSIS OF A SERIES RLC DISCHARGE CIRCUIT

The type of pulse generator used in the conductive mix study was of the RLC, series-discharge type, Figure 1. The effect of the coaxial cable in such a circuit is predominantly inductive, neglecting the very early effects of cable reflections and spark loading of the cable. The capacitance of the cable and stray inductance and capacitance are assumed to cause only secondary effects and are neglected here.

The differential equation for the discharge of a series RLC circuit is

$$Ri + L\frac{di}{dt} + \frac{q}{C} = 0, \qquad (A1)$$

or, the equivalent,

$$R\frac{dq}{dt} + L\frac{d^2q}{dt^2} + \frac{q}{C} = 0, \qquad (A2)$$

where i = current and q = charge (8). These equations simply state that the sum of the three voltage components is equal to zero. Differentiating (A1) gives

$$R\frac{di}{dt} + L\frac{d^2i}{dt^2} + \frac{1}{C} = 0. \qquad (A3)$$

The general solution to equation (A3) is

$$i = \frac{E}{bL}\exp\left\{-at\right\} \cdot \frac{\exp\{bt\} - \exp\{-bt\}}{2} \qquad (A4)$$

where E = initial voltage,

$$a = \frac{R}{2L} \qquad (A5)$$

and

$$b = \sqrt{\frac{R^2}{4L^2} - \frac{1}{LC}} \qquad (A6)$$

There are three forms of the solution and the derivatives depending on the value of R:

a) For the under-damped circuit $\left(R^2 < \frac{4L}{C}\right)$;

$$i = \frac{E}{\beta L} \exp\left\{-at\right\} \cdot \sin \beta t, \tag{A7}$$

$$\frac{di}{dt} = \frac{E}{\beta L} \cdot \exp\left\{-at\right\} \cdot (\beta \cos \beta t - a \sin \beta t), \tag{A8}$$

and

$$\beta = 2\pi f = \sqrt{\frac{1}{LC} - \frac{R^2}{4L^2}}\ , \tag{A9}$$

where f is the frequency. The expression for β, a real quantity, is obtained by rearranging equation (A6), i.e.

$$b = j\sqrt{\frac{1}{LC} - \frac{R^2}{4L^2}} = j\beta\ ,$$

where j is $\sqrt{-1}$.

b) For the critically damped circuit $\left(R^2 = \frac{4L}{C}\right)$;

$$i = \frac{E}{L} t \cdot \exp\left\{-at\right\} \tag{A11}*$$

and

$$\frac{di}{dt} = \frac{E}{L} \exp\left\{-at\right\} \cdot (1 - at)\ . \tag{A12}$$

c) For the over-damped circuit $\left(R^2 > \frac{4L}{C}\right)$;

$$i = \frac{E}{bL} \exp\left\{-at\right\} \cdot \sinh bt \tag{A13}$$

and

$$\frac{di}{dt} = \frac{E}{bL} \exp\left\{-at\right\} (b \cosh bt - a \sinh bt)\ . \tag{A14}$$

From these equations it is seen that the initial rate of rise of current is governed only by E and L, i.e. $di/dt = E/L$ at $t = 0$ for all three cases.

*This expression is obtained by using L' Hospital's rule, since Equation (A6) is in an indeterminant form when $b = 0$.

By setting di/dt = 0 in Equations (A8), (A12) and (A14), the time to reach maximum current ($t_{i\ max}$) is obtained for the under-damped, critically-damped and over-damped cases, respectively:

$$t_{i\ max} = \frac{1}{\beta} \arctan \frac{\beta}{a} , \tag{A15}$$

$$t_{i\ max} = \frac{1}{a} , \tag{A16}$$

and

$$t_{i\ max} = \frac{1}{b} \operatorname{arctanh} \frac{b}{a} . \tag{A17}$$

These equations come from the expressions within the parentheses. The value of the quantity within the parentheses in each case is equal to zero, since the factors outside the parentheses, containing $\exp\{-at\}$, can never be zero within a finite time.

Since the interest in this study is mostly in the under-damped circuit, the expressions of voltage, power and energy for the inductance, capacitance and resistance are given below for this particular case. The solution to Equation (A2), which is required in the analysis, is

$$q = q_o \left(1 - \frac{R^2C}{4L}\right)^{-1/2} \cdot \exp\{-at\} \sin(\beta t + \sigma) , \tag{A18}$$

where q_o = initial charge on the capacitor and $\sigma = \arctan \beta/a$, (9). The expressions for the three voltage components, derived from Equations (A7), (A8), and (A18) are:

$$e_R = iR = \frac{RE}{\beta L} \exp\{-at\} \sin \beta t , \tag{A19}$$

$$e_L = -L \frac{di}{dt} = -\frac{E}{\beta} \exp\{-at\} (\beta \cos \beta t - a \sin \beta t) \tag{A20}$$

and

$$e_C = \frac{q}{C} = \frac{q_o}{C} \left(1 - \frac{R^2C}{4L}\right)^{-1/2} \exp\{-at\} \sin(\beta t + \sigma) , \tag{A21}$$

where $\frac{q_o}{C} = E$, the initial voltage.

The total power of the circuit at any instant is equal to zero, i.e.

$$P = p_R + p_L + p_C = 0 \quad . \tag{A22}$$

The instantaneous power developed in each of the three components is found by multiplying the corresponding voltage expression by the instantaneous current, i,

$$P = i\,(e_R + e_L + e_C) = 0 \quad . \tag{A23}$$

The power generated in the circuit resistance is then

$$p_R = ie_R = i^2R \quad . \tag{A24}$$

The power delivered to the magnetic field is

$$p_L = ie_L = -\,iL\,\frac{di}{dt} \quad . \tag{A25}$$

The power delivered to the electrostatic field is

$$p_C = ie_C = i\,\frac{q}{C} \quad . \tag{A26}$$

The total available energy, W, is expressed as

$$W = \frac{1}{2}\,CE^2 = w_R + w_L + w_C \quad . \tag{A27}$$

The expressions for the energy, w, stored or dissipated in each of the three circuit components are obtained from the following relations:

$$*w_R = W - (w_L - w_C) \quad , \tag{A28}$$

$$w_L = \frac{1}{2}\,L\,i^2 \quad , \tag{A29}$$

and

$$w_C = \frac{1}{2}\,C\,e_C^{\,2} \quad . \tag{A30}$$

---

*w_R may also be found by integrating the corresponding power curve, derived from Equation (A24), (Figure 8).

TABLE I

Resistance (R), inductive impedance (Z_L), and inductance (L) of a 7.6-meter length of type C coaxial cable as a function of frequency (f).

f (Mc)	$\sqrt{f}$	Z_L (ohm)	R (ohm)	L (microh)
0.000	0.000	0.0	0.22	--
*0.540	0.735	6.8	0.41	2.02
0.750	0.866	8.4	0.67	1.77
1.000	1.000	10.5	0.83	1.67
1.500	1.225	15.5	1.17	1.68
2.000	1.410	21.5	1.43	1.72
2.500	1.580	28.5	1.93	1.82
3.000	1.730	36.7	2.72	1.95

*Lower limit on R-F bridge.

TABLE II

Experimental values of the half-period ($\tau/2$), time to reach maximum current ($t_{i\ max}$), and the maximum current (i_{max}) for the conductive mix circuit with 7.6- and 15.2-meter lengths of coaxial cable.

7.6 meters:

Print No.	$\tau/2$ (microsec)	$t_{i\ max}$ (microsec)	i_{max} (amp)
1174	4.81	2.05	2430
1176b)	4.80	2.02	2470
1176c)	4.80	2.02	2420
1177a)	4.81	2.04	2360
1177b)	4.77	2.02	2375
1178a)	4.79	2.04	2430
1178b)	4.81	2.04	2430
Average:	4.80	2.03	2420

15.2 meters:

Print No.	$\tau/2$ (microsec)	$t_{i\ max}$ (microsec)	i_{max} (amp)
1176b)	6.25	2.65	1830
1176c)	6.28	2.65	1830
1177a)	6.26	2.61	1740
1177b)	6.18	2.64	1740
1178a)	6.27	2.64	1750
Average:	6.25	2.64	1778

TABLE III

Frequency of oscillation (f), maximum current (i_{max}), and time to reach maximum current ($t_{i\ max}$) as a function of total circuit resistance (R).

R (ohm)	f (Mc)*	$t_{i\ max}$ (microsec)	i_{max} (amp)
0.6	0.10519	2.0732	2513.5
0.7	0.10440	2.0370	2413.1
**0.721	0.10421	2.0296	2392.9
0.8	0.10348	2.0023	2319.9
0.9	0.10243	1.9690	2233.0
1.0	0.10124	1.9370	2152.0
1.1	0.09992	1.9064	2076.2
1.2	0.09844	1.8767	2005.4
1.3	0.09682	1.8486	1938.7
1.4	0.09503	1.8208	1876.3
1.5	0.09307	1.7993	1814.4
1.6	0.09093	1.7688	1761.8

* This is the frequency that would exist if the circuit were allowed to oscillate.
** Value of R without spark.

TABLE IV

Resistance of conductive mix spark and maximum current through the spark as a function of gap width (initial voltage 5.00 kv).

A. Sugar/aluminum (97/3), copper electrodes with 30° tips.

Gap Width (mm)	Density (g/cm^3)	Observed Peak Current (amp)	Calculated Resistance (ohm)
0.10	0.9	2266	0.14
0.36	0.7	2174	0.25
0.45	0.9	2240	0.17
0.76	0.7	2174	0.25
0.89	0.7	2184	0.24
1.07	0.9	2127	0.31
1.34	0.7	2123	0.32
1.49	0.9	2113	0.33
2.10	No discharge	--	--
2.79	No discharge	--	--

B. Sugar/aluminum (97/3), copper electrodes with 30° tips, aluminum paint in gap.

Gap Width (mm)	Density (g/cm^3)	Observed Peak Current (amp)	Calculated Resistance (ohm)
0.10	0.9	2226	0.19
0.30	0.7	2219	0.20
0.34	0.9	2211	0.21
0.91	0.9	2157	0.28
0.94	0.7	2174	0.25
1.30	0.9	2143	0.29
1.36	0.7	2148	0.29
2.10	0.9	2058	0.41
2.79	0.9	2001	0.49

TABLE IV
(cont.)

C. Sugar/aluminum (97/3), aluminum electrodes with 30° tips.

Gap Width (mm)	Density (g/cm^3)	Observed Peak Current (amp)	Calculated Resistance (ohm)
0.21	0.7	2224	0.19
0.41	0.7	2224	0.19
0.56	0.7	2249	0.16
3.05	0.7	2033	0.44
3.18	0.7	1937	0.58

D. RDX/aluminum (97/3), copper electrodes with 30° tips.

Gap Width (mm)	Density (g/cm^3)	Observed Peak Current (amp)	Calculated Resistance (ohm)
0.51	0.9	2290	0.11
0.51	0.9	2235	0.18
0.51	1.2	2233	0.18
0.51	1.2	2233	0.18

E. RDX/aluminum (97/3), aluminum electrodes with 30° tips.

Gap Width (mm)	Density (g/cm^3)	Observed Peak Current (amp)	Calculated Resistance (ohm)
0.76	0.8	2169	0.26
0.76	0.8	2137	0.30
0.76	0.8	2160	0.27
0.76	0.8	2075	0.38

TABLE IV
(cont.)

F. Sugar/aluminum (97/3), copper electrodes with 120° tips.

Gap Width (mm)	Density (g/cm^3)	Observed Peak Current (amp)	Calculated Resistance (ohm)
0.19	0.9	2302	0.10
0.25	0.9	2320	0.08
0.80	0.9	2280	0.12
1.13	0.9	2204	0.22
1.59	0.9	2181	0.25
2.92	0.9	No Discharge	--

TABLE V

Calculated current and voltages as a function of time in circuit used for conductive mix tests. (C = 0.985 mfd, L = 2.232 microh, E = 5.00 kv, and R = 0.900 ohm.)

Time (microsec)	Current (amp)	Voltage (volt)		
t	i	e_R	e_L	e_C
0.0	0.0	0.0	5000.0	-5000.0
0.5	996.0	896.4	3843.4	-4739.9
1.0	1707.3	1536.6	2501.2	-4037.8
1.5	2115.2	1903.7	1151.1	-3054.8
*1.9690	2233.3	2010.0	0.0	-2009.9
2.0	2232.8	2009.5	- 69.9	-1939.6
2.5	2101.2	1891.1	-1060.8	- 830.2
3.0	1779.2	1601.3	-1762.6	161.3
3.5	1334.6	1201.1	-2156.4	955.4
4.0	834.9	751.5	-2258.4	1506.9
4.5	341.4	307.2	-2111.3	1804.1
5.0	- 96.9	- 87.2	-1775.7	1862.9
5.5	- 445.3	- 400.8	-1320.1	1721.0

*Time to reach maximum current, $t_{i\,(max)}$.

TABLE VI

Calculated instantaneous power as a function of time for R, L, and C. (Values of circuit parameter are the same as for Table V.)

Time (microsec)	Instantaneous Power (megawatts)		
t	i^2R	$iL\frac{di}{dt}$	$i\frac{q}{C}$
0.0	0.0000	0.0000	0.0000
0.5	0.8928	3.8281	-4.7210
1.0	2.6235	4.2703	-6.8938
1.5	4.0267	2.4348	-6.4614
*1.9690	4.4888	0.0000	-4.4887
2.0	4.4869	-0.1560	-4.3308
2.5	3.9734	-2.2289	-1.7444
3.0	2.8490	-3.1360	0.2870
3.5	1.6030	-2.8779	1.2750
4.0	0.6274	-1.8856	1.2582
4.5	0.1049	-0.7207	0.6159
5.0	0.0085	0.1721	-0.1805
5.5	0.1785	0.5879	-0.7664

* t_1 (max)

TABLE VII

Calculated energy distribution as a function of time for R, L, and C. (Values of circuit parameters are the same as for Table V.)

Time (microsec)	Energy (joule)		
t	Dissipated by R**	$\frac{1}{2} Li^2$	$\frac{1}{2} Ce_C^2$
0.0	0.0000	0.0000	12.3125
0.5	0.1408	1.1071	11.0646
1.0	1.0299	3.2531	8.0295
1.5	2.7237	4.9931	4.5958
*1.9690	4.7567	5.5662	1.9896
2.0	4.8960	5.5637	1.8528
2.5	7.0460	4.9271	0.3395
3.0	8.7669	3.5328	0.0128
3.5	9.8753	1.9877	0.4495
4.0	10.4161	0.7780	1.1184
4.5	10.5795	0.1301	1.6029
5.0	10.5928	0.0105	1.7093
5.5	10.6325	0.2213	1.4587

* t_i (max)
**Total circuit resistance, including spark. (R = 0.900 ohm)

TABLE VIII

Calculated power and energy of a spark within a typical conductive mix as a function of time.

Time (microsec)	Power (megawatt)	Energy (joule)
0.0	0.0000	0.0000
0.5	0.1776	0.0280
1.0	0.5218	0.2048
1.5	0.8009	0.5417
*1.9690	**0.8928	0.9373
2.0	0.8924	0.9738
2.5	0.7903	1.4014
3.0	0.5666	1.7436
3.5	0.3188	1.9641
4.0	0.1248	2.0717
4.5	0.0209	2.1042
5.0	0.0017	2.1068
5.5	0.0355	2.1147

* t_i (max)
**peak power

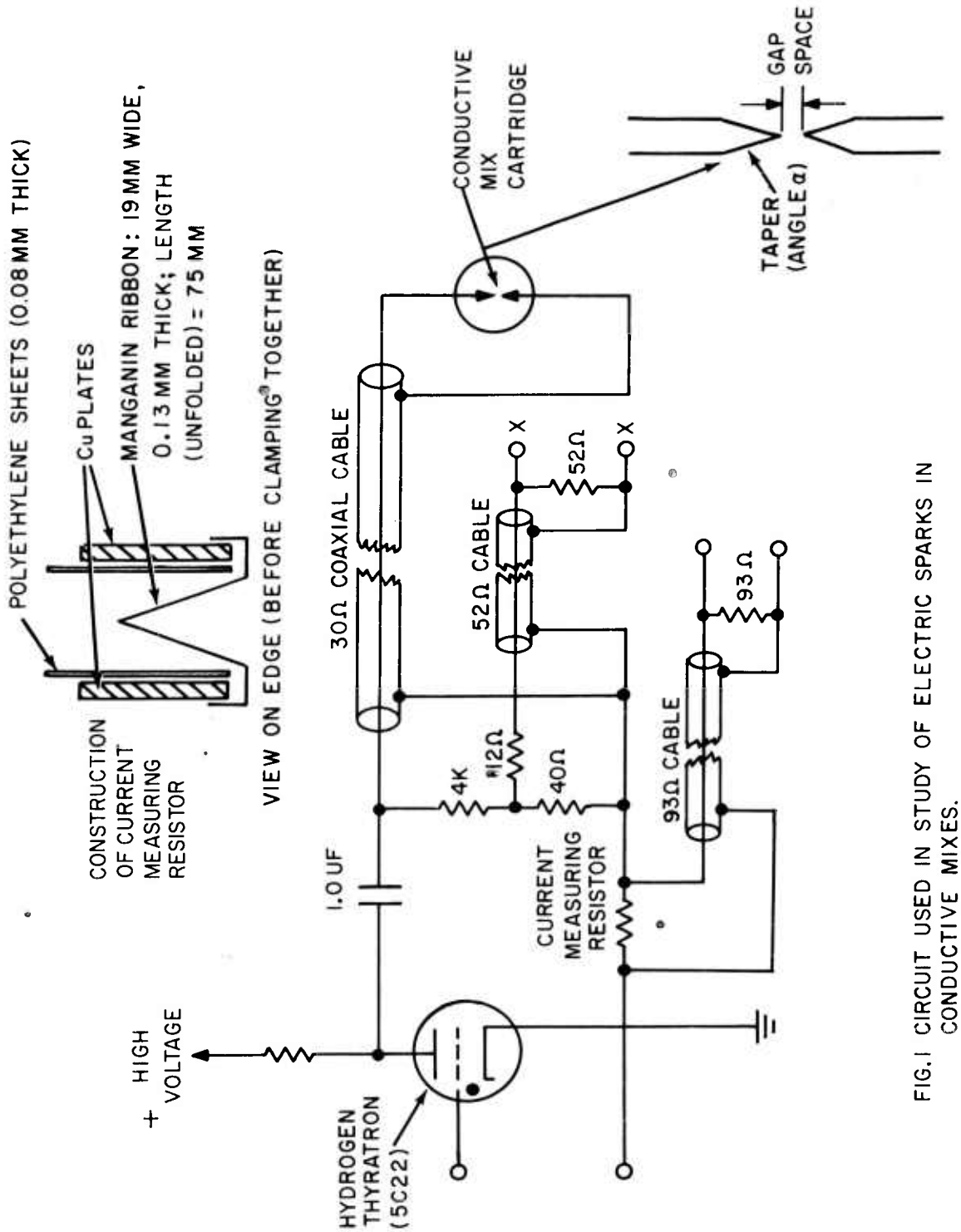

FIG. 1 CIRCUIT USED IN STUDY OF ELECTRIC SPARKS IN CONDUCTIVE MIXES.

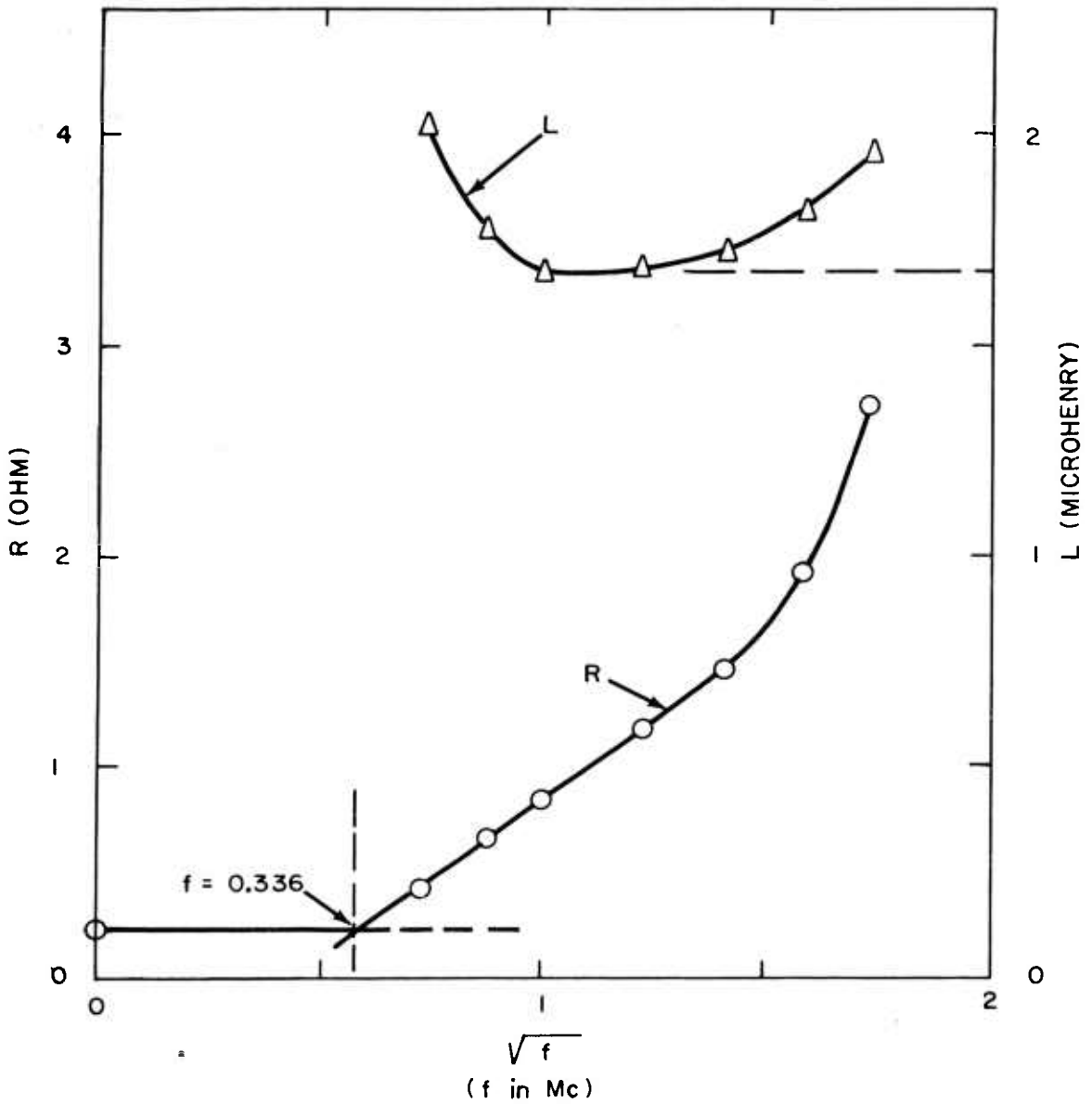

FIG. 2 RESISTANCE AND INDUCTANCE AS A FUNCTION OF THE SQUARE ROOT OF THE FREQUENCY FOR 7.6 METERS OF TYPE C COAXIAL CABLE.

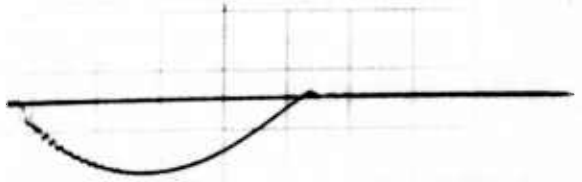

(A) TYPICAL CURRENT VS. TIME RECORD.

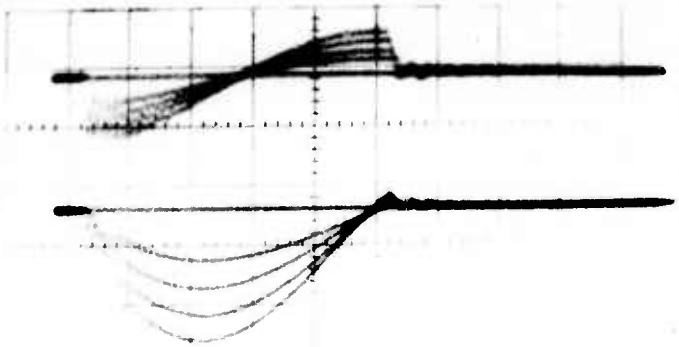

(B) SIMULTANEOUS VOLTAGE AND CURRENT RECORDS VS. TIME FOR 7.6-METER COAXIAL CABLE WITH INITIAL VOLTAGES OF 2,3,4, AND 5 KV.

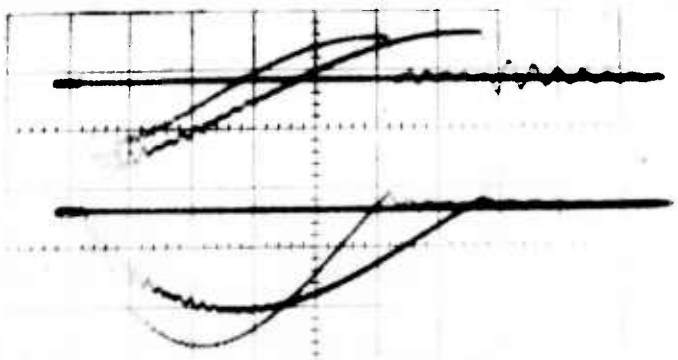

(C) SIMULTANEOUS VOLTAGE AND CURRENT RECORDS VS. TIME FOR 7.6-AND 15.2-METER COAXIAL CABLE. INITIAL VOLTAGE: 5KV.

(D) CURRENT VS. TIME RECORD SHOWING OCCASIONAL OSCILLATORY NATURE OF THE DISCHARGE WHEN THE THYRATRON FUNCTIONS IMPROPERLY.

FIG. 3 TYPICAL OSCILLOSCOPE TRACES OF CURRENTS AND VOLTAGES. HORIZONTAL SCALE: 1.0 MICROSEC PER DIVISION.

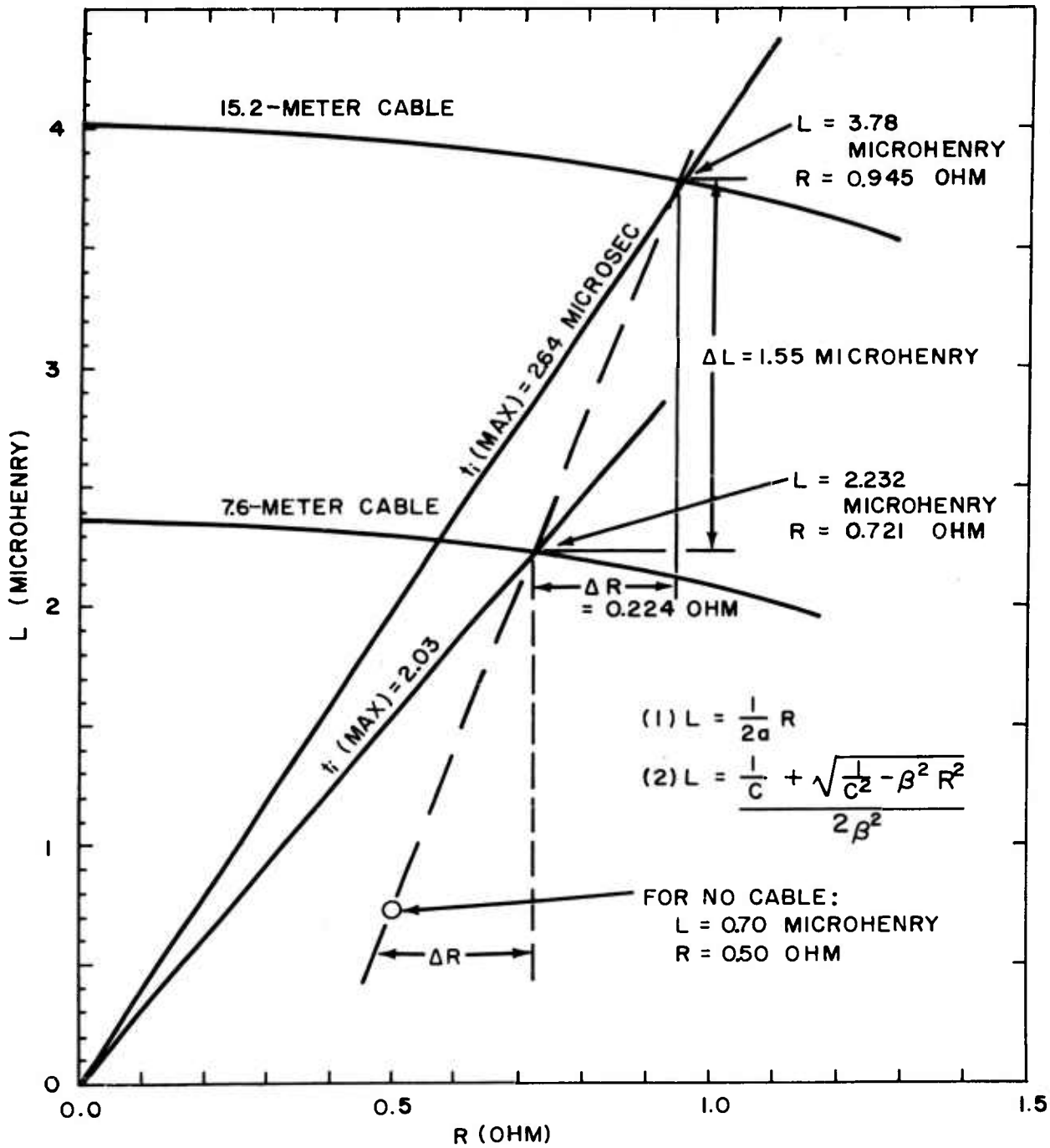

FIG. 4 GRAPHICAL SOLUTIONS OF L AND R FROM EQUATIONS (1) AND (2) FOR THE CIRCUIT OF FIG. 1, USING 7.6-AND 15.2-METER COAXIAL CABLES.

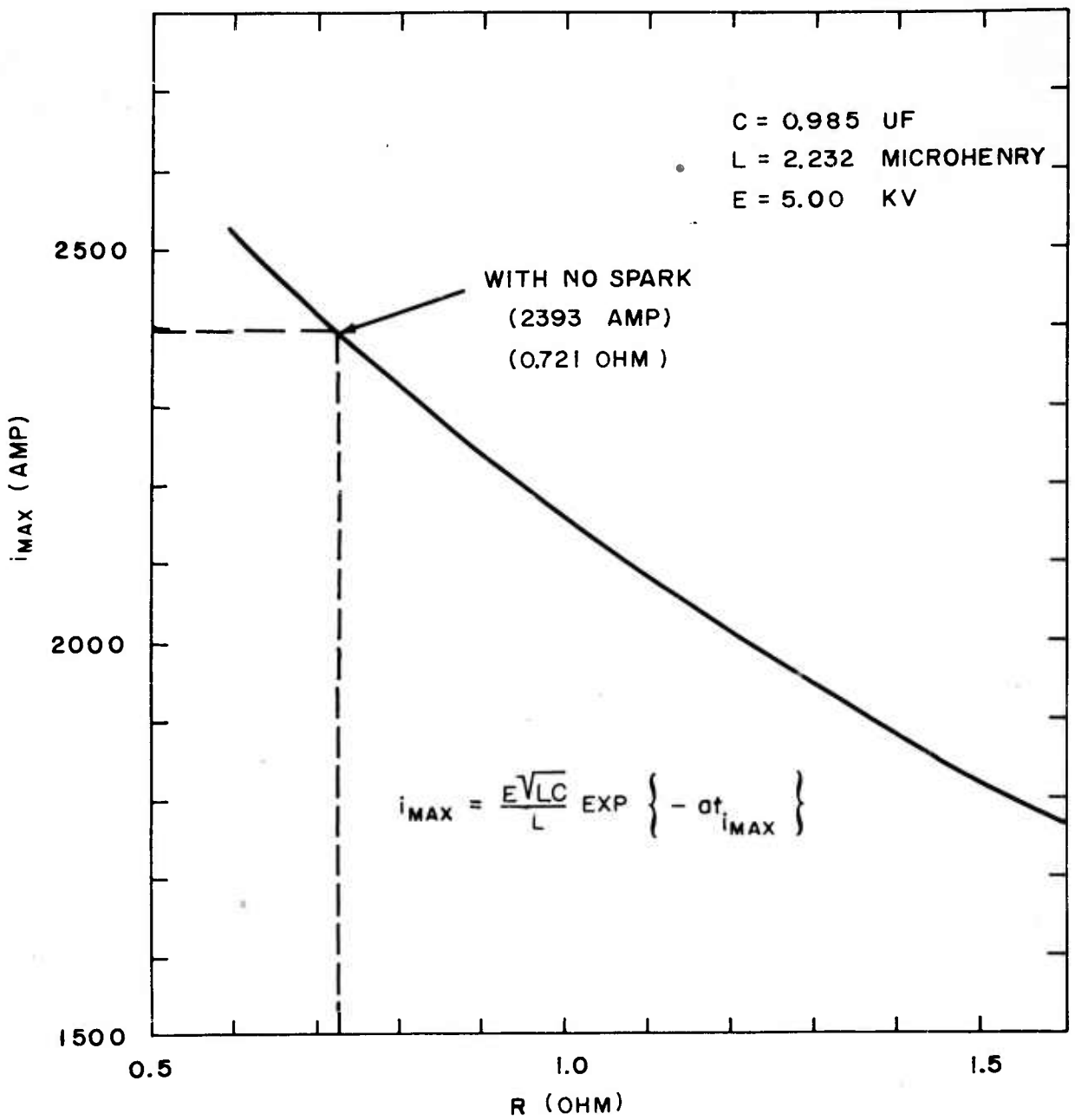

FIG. 5 MAXIMUM CURRENT AS A FUNCTION OF THE TOTAL CIRCUIT RESISTANCE.

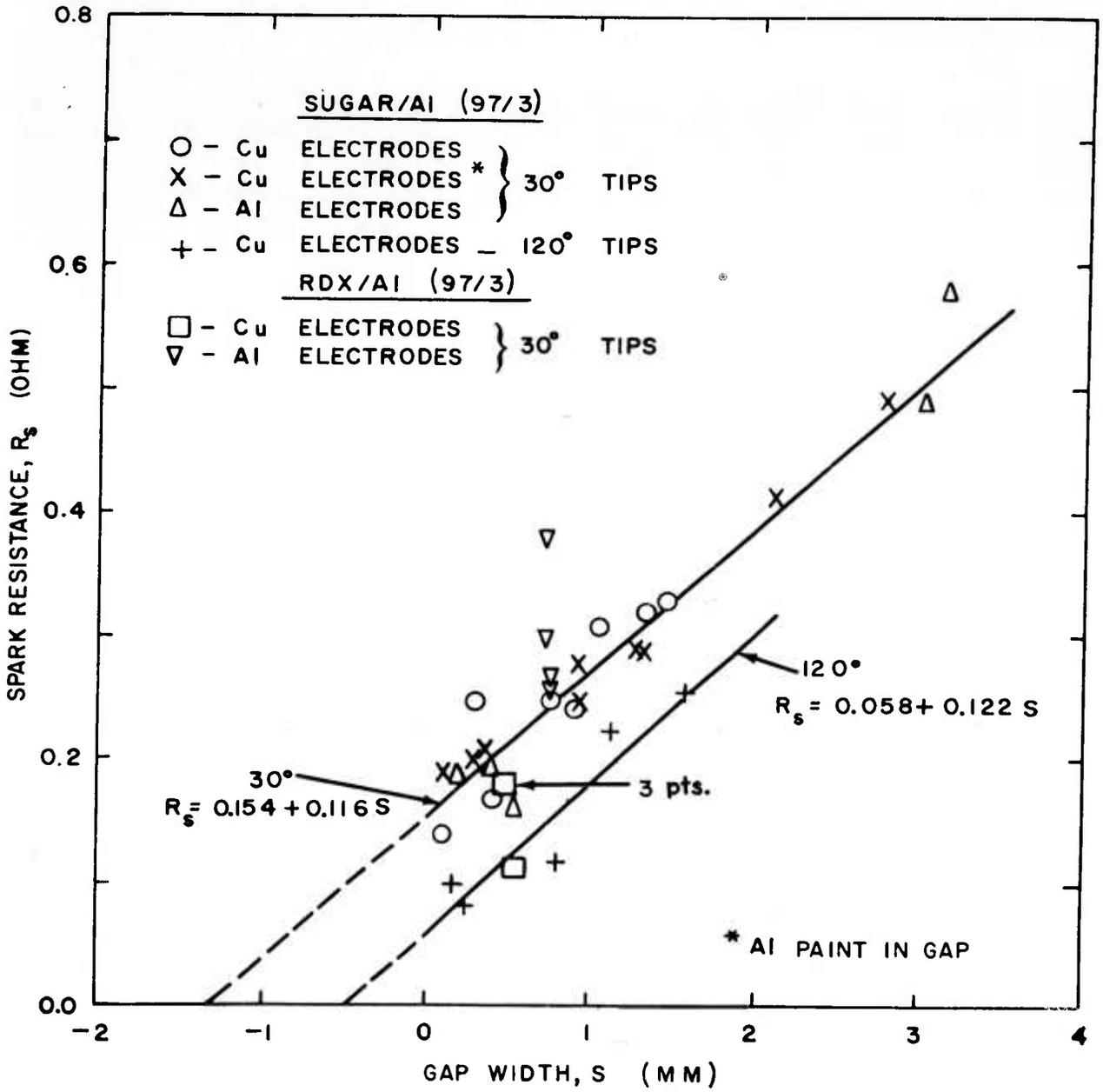

FIG. 6 RESISTANCE OF CONDUCTIVE MIX SPARKS AS A FUNCTION OF THE ELECTRODE GAP WIDTH. (DENSITIES WERE 0.7, 0.9 AND 1.2 g/ cm^3— SEE TABLE IV.)

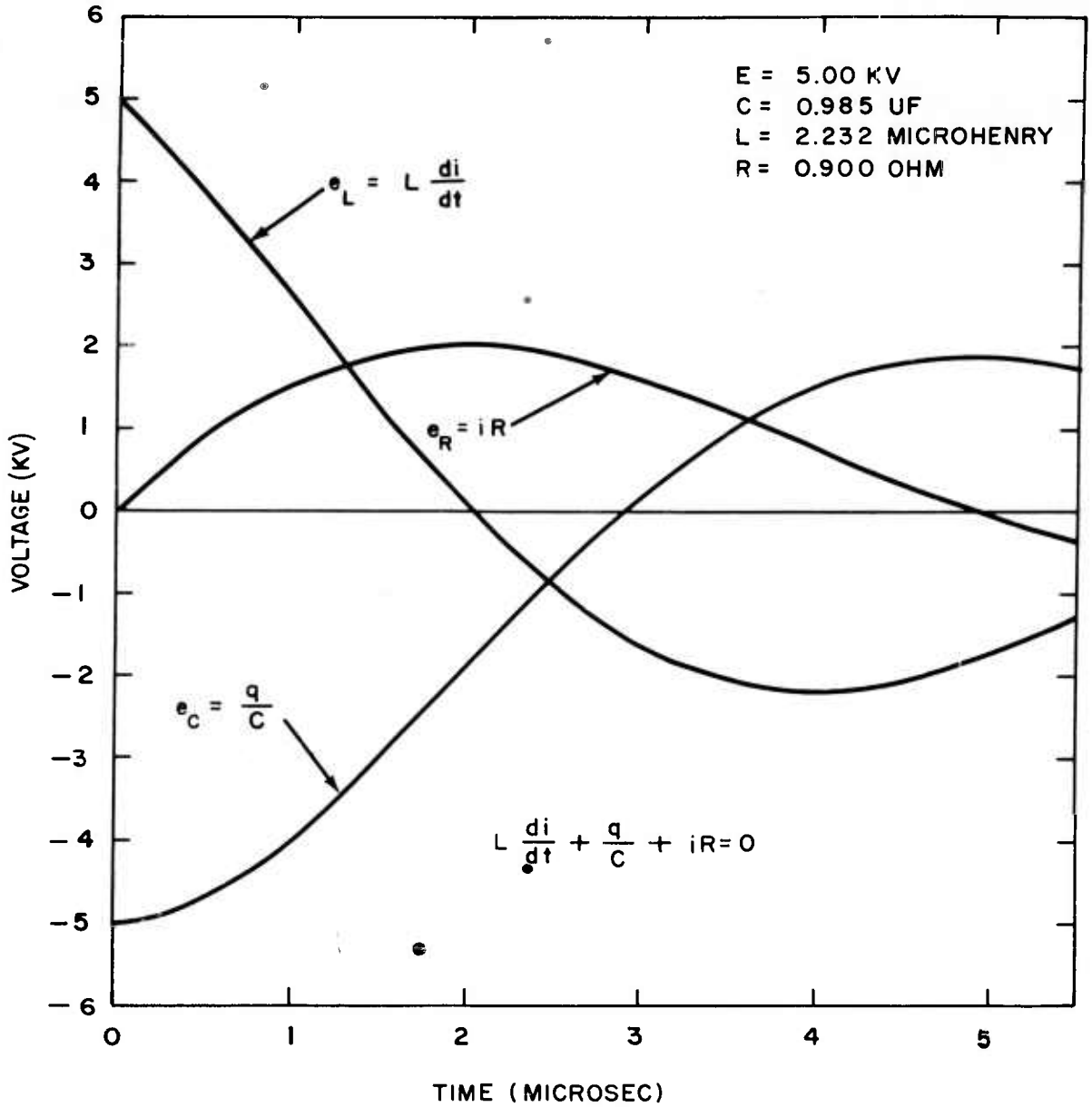

FIG. 7 VOLTAGES ACROSS THE RESISTANCE, SELF-INDUCTANCE, AND CAPACITANCE OF A SERIES LCR DISCHARGE CIRCUIT AS A FUNCTION OF TIME.

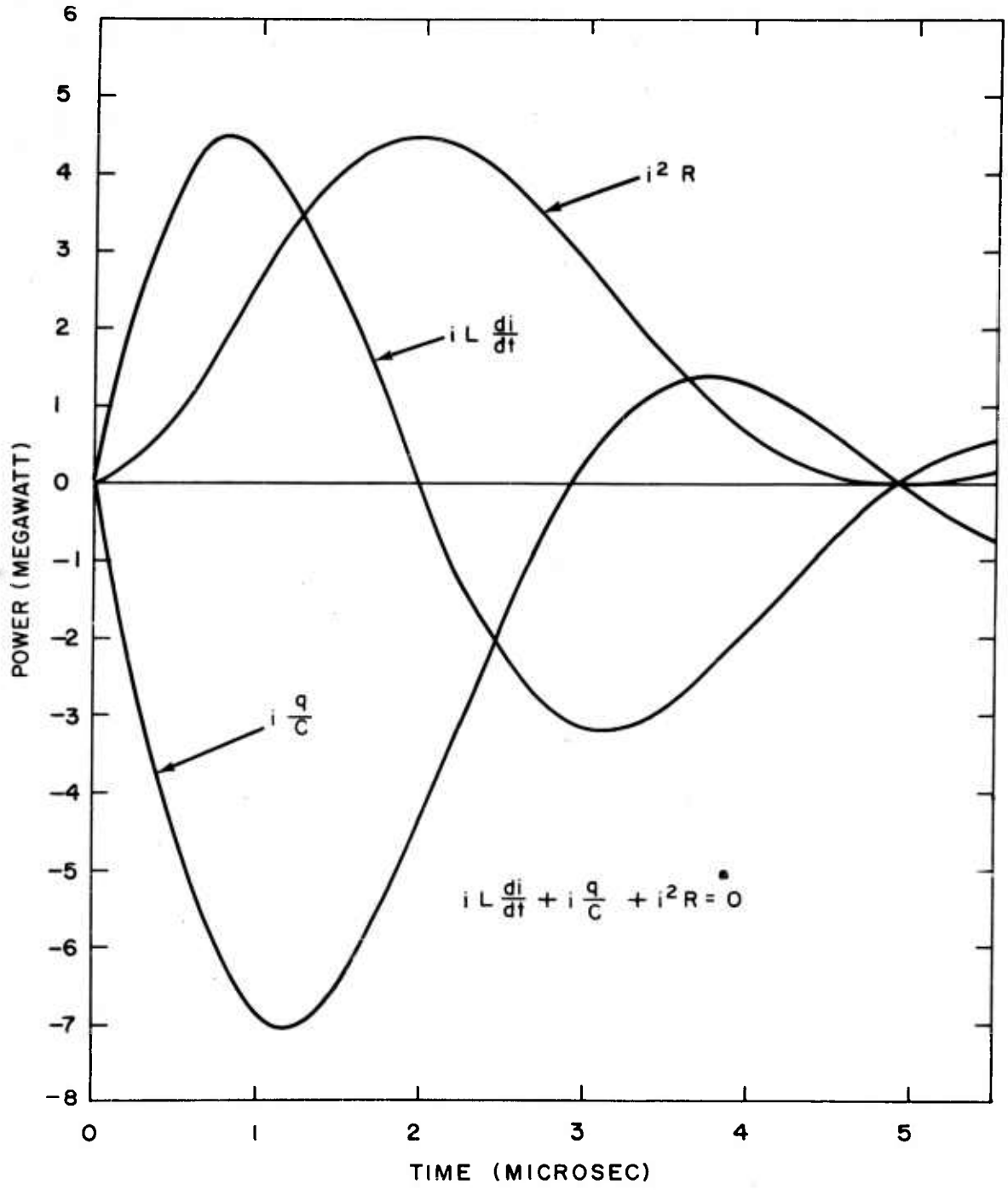

FIG. 8 INSTANTANEOUS POWER AS A FUNCTION OF TIME, CORRESPONDING TO THE CIRCUIT VALUES GIVEN IN FIG.7

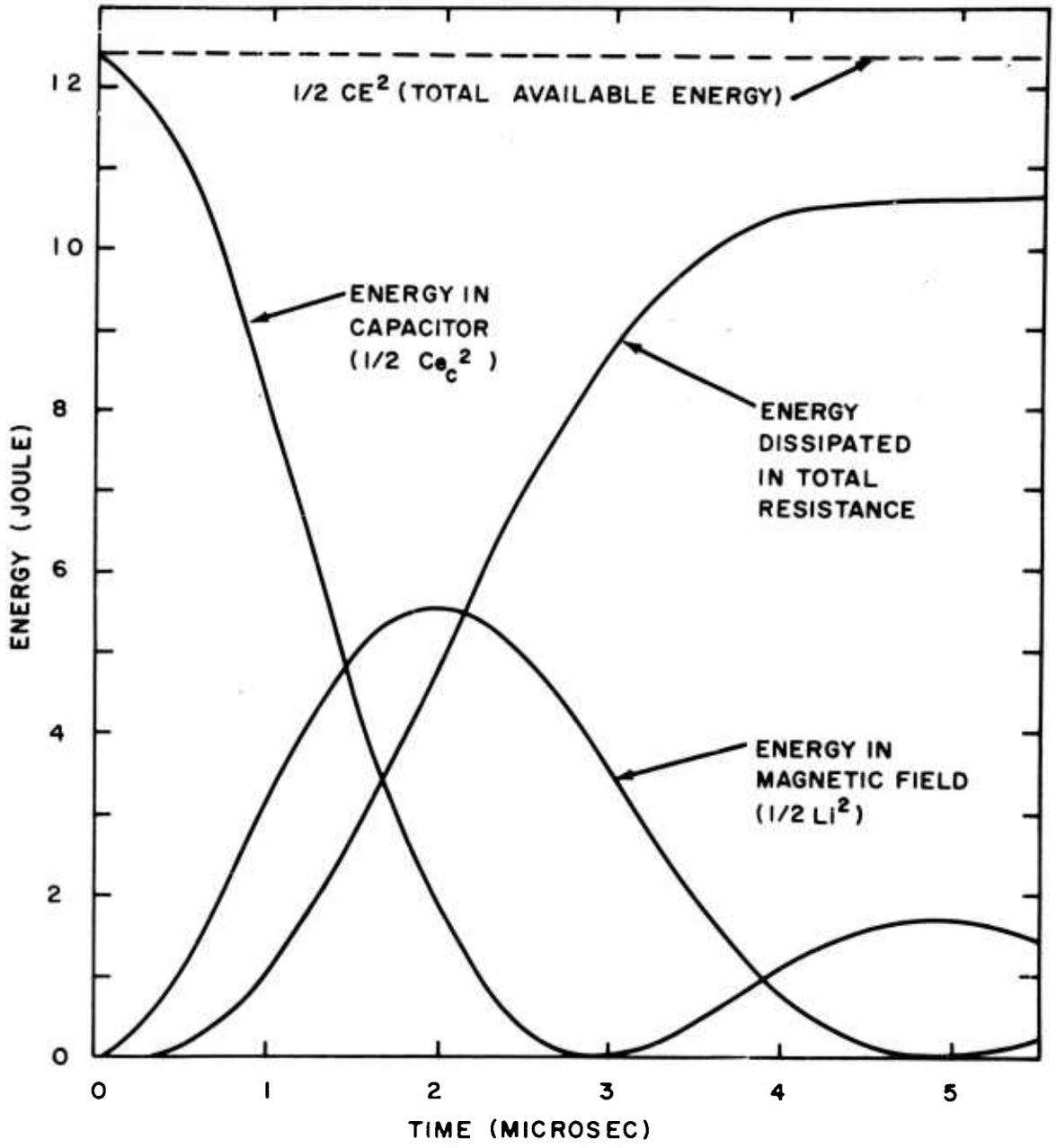

FIG. 9 ENERGY DISTRIBUTION AS A FUNCTION OF TIME, CORRESPONDING TO THE CIRCUIT VALUES GIVEN IN FIG. 7

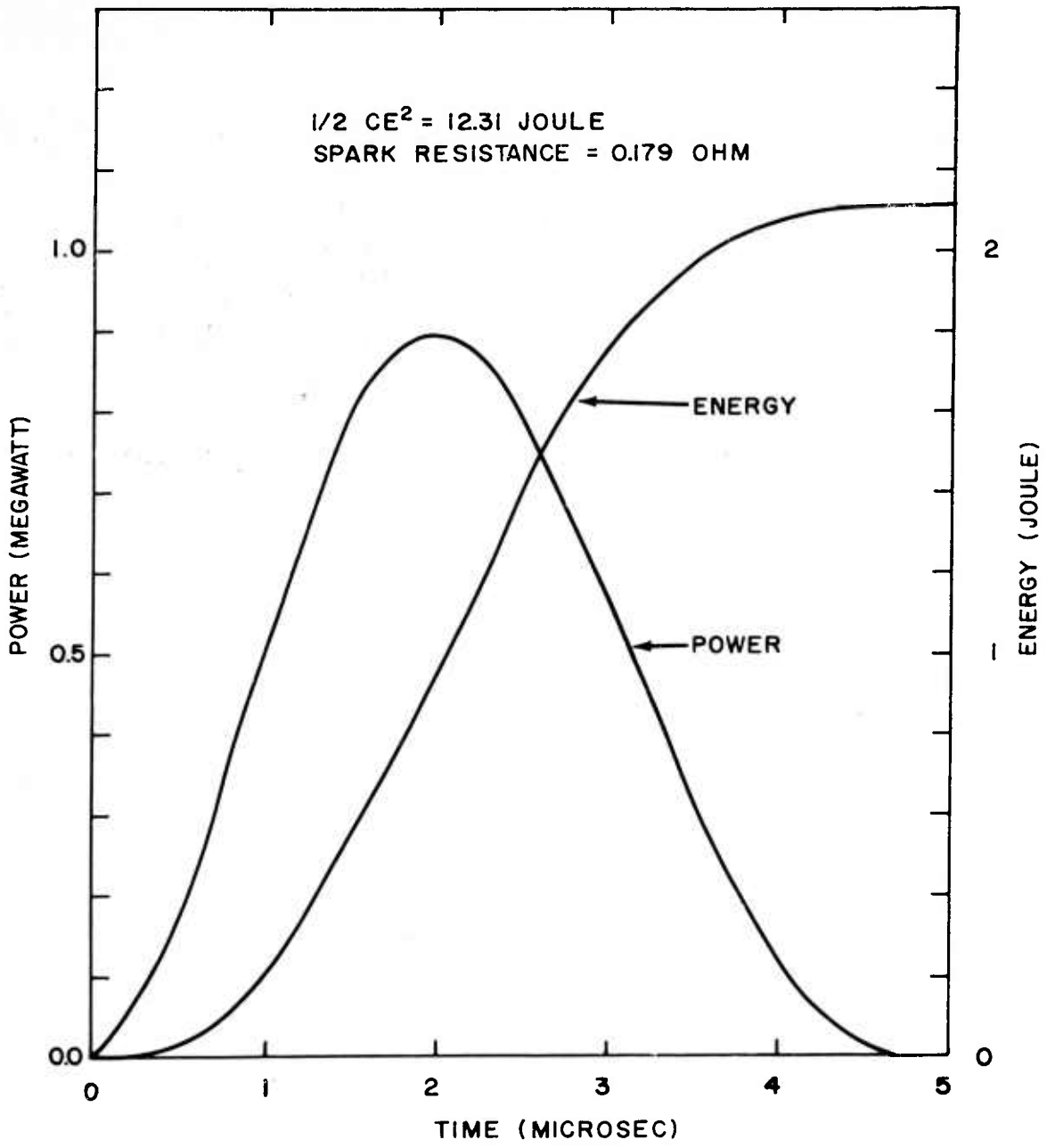

FIG. 10 INSTANTANEOUS POWER AND ACCUMULATED ENERGY FOR A SPARK WITHIN A TYPICAL CONDUCTIVE MIX AS A FUNCTION OF TIME, CORRESPONDING TO THE CIRCUIT VALUES GIVEN IN FIG. 7.

DISTRIBUTION LIST

	Copies
Chief, Bureau of Naval Weapons Department of the Navy Washington 25, D. C.	
DIS-32	2
RRRE-5	1
RUME-11	1
RUME-32	1
RMMO-2	1
RREN-312	1
Director, Special Projects Office Department of the Navy Washington 25, D. C.	
SP 20	1
Chief, Bureau of Ships Department of the Navy Washington 25, D. C.	
Code 423	1
Chief of Naval Research Department of the Navy Washington 25, D. C.	
Chemistry Branch	2
Commandant U. S. Marine Corps Washington 25, D. C.	1
Commander, U. S. Naval Ordnance Test Station China Lake, California	
Code 556	1
Code 4572	1
Technical Library	2
B. A. Breslow	1
J. Sherman	1
Director, Naval Research Laboratory Washington 25, D. C.	
Technical Information Section	2
Superintendent, Naval Post Graduate School Monterey, California	1

DISTRIBUTION LIST (Cont'd.)

	Copies
Commander, Naval Air Development Center Johnsville, Pennsylvania Aviation Armament Laboratory	1
Commander, U. S. Naval Weapons Laboratory Dahlgren, Virginia Technical Library	2
Weapons Laboratory	1
Terminal Ballistics Laboratory	1
Commanding Officer, U. S. Naval Weapons Station Yorktown, Virginia R & D Division	2
Commanding Officer, U. S. Naval Ordnance Laboratory Corona, California	2
Commanding Officer, U. S. Naval Propellant Plant Indian Head, Maryland Technical Library	1
EODTC	1
Commander, U. S. Navy Electronics Laboratory San Diego, California	1
Commander, Naval Radiological Defense Laboratory San Francisco, California Ruth Schnider	1
Commanding Officer, U. S. Naval Ammunition Depot Navy Number Six Six (66) c/o Fleet Post Office San Francisco, California Quality Evaluation Laboratory	1
Commanding Officer, Naval Ammunition Depot Crane, Indiana	1
Commanding Officer, U. S. Naval Weapons Evaluation Unit Kirtland Air Force Base Albuquerque, New Mexico	1
Office of Chief of Ordnance Department of the Army Washington 25, D. C. ORDGU	1
ORDTB	1
ORDTN	1

DISTRIBUTION LIST (Cont'd.)

	Copies
Commander, Army Rocket and Guided Missile Agency Redstone Arsenal, Alabama	
ORDXR-RH	1
Commanding General, Picatinny Arsenal Dover, New Jersey	
ORDBB-TH8, Technical Information	1
ORDBB-TJ1, H.E. Section	1
ORDBB-TK3, Prop. and Expl. Unit	1
ORDBB-TM1, Chem. Res. Section	1
ORDBB-TP1, Proj. Fuze Section	1
ORDBB-TP2, GM, Rkt. and Bomb Fuze	1
ORDBB-TP3, Init. and Spec. Dev.	2
ORDBB-TR2, Phys. Res. Section	1
ORDBB-TS1, Pyrotech. Lab.	1
Commanding Officer, Diamond Ordnance Fuze Laboratory Connecticut Avenue & Van Ness St., N.W. Washington 25, D. C.	
Ordnance Development Laboratory	1
M. Lipnick (Code 005)	1
Commanding Officer, Office of Ordnance Research Box CM, Duke Station Durham, North Carolina	1
Commanding General, Frankfort Arsenal Philadelphia 37, Pennsylvania	1
Commanding General, U. S. Army Proving Ground Aberdeen, Maryland	
Technical Library	1
Dr. R. J. Eichelberger	1
M. Sultanoff	1
Office of Chief of Engineers Department of the Army Washington 25, D. C.	1
Commanding Officer Engineer Research & Development Laboratory U. S. Army Ft. Belvoir, Virginia	
Technical Intelligence Branch	1
Commanding General, White Sands Proving Ground White Sands, New Mexico	1

DISTRIBUTION LIST (Cont'd.)

	Copies
Chief of Staff U. S. Air Force Washington 25, D. C. AFORD-AR	1
Commander, Wright Air Development Center Wright-Patterson Air Force Base Dayton, Ohio	1
WWAD	2
Hdqts., Air Proving Ground Center U. S. Air Force, ARDC Eglin Air Force Base, Florida	1
PGTRI, Technical Library	1
Commander, Air Research & Development Command Andrews Air Force Base Washington 25, D. C.	1
Commander, Rome Air Development Center Griffiss Air Force Base Rome, New York	1
Commander, Air Force Cambridge Research Center L. G. Hanscom Field Bedford, Massachusetts	1
Chief, Defense Atomic Support Agency Washington 25, D. C.	5
Armed Services Technical Information Agency Arlington Hall Station Arlington 12, Virginia	10
Director, U. S. Bureau of Mines Division of Explosive Technology 4800 Forbes Street Pittsburgh 13, Pennsylvania Dr. R. W. Van Dolah	1
Atomic Energy Commission Washington 25, D. C. DMA	1
National Aeronautics & Space Administration Headquarters 1520 H Street, N.W. Washington 25, D. C.	1

DISTRIBUTION LIST (Cont'd.)

	Copies
National Aeronautics & Space Administration Goddard Space Flight Center Greenbelt, Maryland	1
Lewis Research Center, N.A.S.A. 21,000 Brookpark Road Cleveland 35, Ohio Library	1
Director, USAF Project RAND (Via USAF Liaison Office) The RAND Corporation 1700 Main Street Santa Monica, California Librarian	1
Lawrence Radiation Laboratory University of California P. O. Box 808 Livermore, California	
Technical Information Division	1
Dr. C. Godfrey	1
Dr. J. Kury	1
Director, Los Alamos Scientific Laboratory P. O. Box 1663 Los Alamos, New Mexico Library	1
Sandia Corporation P. O. Box 969 Livermore, California	1
Sandia Corporation P. O. Box 5400 Albuquerque, New Mexico	1
Director, Applied Physics Laboratory John Hopkins University 8621 Georgia Avenue Silver Spring, Maryland	2
Solid Propellants Agency	1
Office of Technical Services Department of Commerce Washington 25, D. C.	100

DISTRIBUTION LIST (Cont'd.)

	Copies
Aerojet-General Corporation Ordnance Division Downey, California Dr. Louis Zernow	1
Alleghany Ballistics Laboratory Cumberland, Maryland	1
Armour Research Foundation Technology Center Illinios Institute of Technology 10 West 35th Street Chicago 16, Illinois	1
The Bendix Corporation Scintilla Division Sidney, New York R. M. Purdy	1
Denver Research Institute University of Denver Denver 10, Colorado	1
E. I. duPont DeNemours Eastern Laboratories Explosives Department Gibbstown, New Jersey Dr. L. Coursen	1
The Franklin Institute 20th Street & Benjamin Franklin Parkway Philadelphia 3, Pennsylvania Project TAL-2707 AA	1
Librascope-Sunnyvale 670 Arques Avenue Sunnyvale, California	1
Lockheed Aircraft Corporation P. O. Box 504 Sunnyvale, California	1
Stanford Research Institute Poulter Laboratories Menlo Park, California	1

DISTRIBUTION LIST (Cont'd.)

	Copies
University of Utah Salt Lake City, Utah Dr. Melvin Cook, Explosive Research Group	1
Vitro Corporation Silver Spring Laboratories 14000 Georgia Avenue Silver Spring, Maryland	1

Naval Ordnance Laboratory, White Oak, Md.
(NOL technical report 61-67)
THE CHARACTERISTICS OF ELECTRIC SPARK DISCHARGES IN MIXTURES OF HIGH-EXPLOSIVE AND ALUMINUM POWDERS (U), by T.P. Liddiard, jr. 25 Aug. 1961. 36p. charts, diagrs. Task NOL-260. Project LACE. UNCLASSIFIED

A method is described for obtaining the average resistance of a spark discharging through a granular conductive mix in a non-oscillating discharge system. The spark resistance is a linear function of the spark gap width for a given electrode arrangement. The resistance is relatively independent of the density of the mix over the range 0.7 to 0.9 ohm.

Abstract card is unclassified

1. Explosives - Initiation
2. Explosives - Detonation
3. Explosive, High
4. RDX/aluminum
5. Sugar/aluminum
I. Title
II. Liddiard, Thomas P.
III. Project
IV. Project

Naval Ordnance Laboratory, White Oak, Md.
(NOL technical report 61-67)
THE CHARACTERISTICS OF ELECTRIC SPARK DISCHARGES IN MIXTURES OF HIGH-EXPLOSIVE AND ALUMINUM POWDERS (U), by T.P. Liddiard, jr. 25 Aug. 1961. 36p. charts, diagrs. Task NOL-260. Project LACE. UNCLASSIFIED

A method is described for obtaining the average resistance of a spark discharging through a granular conductive mix in a non-oscillating discharge system. The spark resistance is a linear function of the spark gap width for a given electrode arrangement. The resistance is relatively independent of the density of the mix over the range 0.7 to 0.9 ohm.

Abstract card is unclassified

1. Explosives - Initiation
2. Explosives - Detonation
3. Explosive, High
4. RDX/aluminum
5. Sugar/aluminum
I. Title
II. Liddiard, Thomas P.
III. Project
IV. Project

Naval Ordnance Laboratory, White Oak, Md.
(NOL technical report 61-67)
THE CHARACTERISTICS OF ELECTRIC SPARK DISCHARGES IN MIXTURES OF HIGH-EXPLOSIVE AND ALUMINUM POWDERS (U), by T.P. Liddiard, jr. 25 Aug. 1961. 36p. charts, diagrs. Task NOL-260. Project LACE. UNCLASSIFIED

A method is described for obtaining the average resistance of a spark discharging through a granular conductive mix in a non-oscillating discharge system. The spark resistance is a linear function of the spark gap width for a given electrode arrangement. The resistance is relatively independent of the density of the mix over the range 0.7 to 0.9 ohm.

Abstract card is unclassified

1. Explosives - Initiation
2. Explosives - Detonation
3. Explosive, High
4. RDX/aluminum
5. Sugar/aluminum
I. Title
II. Liddiard, Thomas P.
III. Project
IV. Project

Naval Ordnance Laboratory, White Oak, Md.
(NOL technical report 61-67)
THE CHARACTERISTICS OF ELECTRIC SPARK DISCHARGES IN MIXTURES OF HIGH-EXPLOSIVE AND ALUMINUM POWDERS (U), by T.P. Liddiard, jr. 25 Aug. 1961. 36p. charts, diagrs. Task NOL-260. Project LACE. UNCLASSIFIED

A method is described for obtaining the average resistance of a spark discharging through a granular conductive mix in a non-oscillating discharge system. The spark resistance is a linear function of the spark gap width for a given electrode arrangement. The resistance is relatively independent of the density of the mix over the range 0.7 to 0.9 ohm.

Abstract card is unclassified

1. Explosives - Initiation
2. Explosives - Detonation
3. Explosive, High
4. RDX/aluminum
5. Sugar/aluminum
I. Title
II. Liddiard, Thomas P.
III. Project
IV. Project

Naval Ordnance Laboratory, White Oak, Md.
(NOL technical report 61-67)
THE CHARACTERISTICS OF ELECTRIC SPARK DISCHARGES IN MIXTURES OF HIGH-EXPLOSIVE AND ALUMINUM POWDERS (U), by T.P. Liddiard, jr. 25 Aug. 1961. 36p. charts, diagrs. Task NOL-260. Project LACE. UNCLASSIFIED

A method is described for obtaining the average resistance of a spark discharging through a granular conductive mix in a non-oscillating discharge system. The spark resistance is a linear function of the spark gap width for a given electrode arrangement. The resistance is relatively independent of the density of the mix over the range 0.7 to 0.9 ohm.

Abstract card is unclassified

1. Explosives - Initiation
2. Explosives - Detonation
3. Explosive, High
4. RDX/aluminum
5. Sugar/aluminu
I. Title
II. Liddiard, Thomas P.
III. Project
IV. Project

Naval Ordnance Laboratory, White Oak, Md.
(NOL technical report 61-67)
THE CHARACTERISTICS OF ELECTRIC SPARK DISCHARGES IN MIXTURES OF HIGH-EXPLOSIVE AND ALUMINUM POWDERS (U), by T.P. Liddiard, jr. 25 Aug. 1961. 36p. charts, diagrs. Task NOL-260. Project LACE. UNCLASSIFIED

A method is described for obtaining the average resistance of a spark discharging through a granular conductive mix in a non-oscillating discharge system. The spark resistance is a linear function of the spark gap width for a given electrode arrangement. The resistance is relatively independent of the density of the mix over the range 0.7 to 0.9 ohm.

Abstract card is unclassified

1. Explosives - Initiation
2. Explosives - Detonation
3. Explosive, High
4. RDX/aluminum
5. Sugar/aluminu
I. Title
II. Liddiard, Thomas P.
III. Project
IV. Project

Naval Ordnance Laboratory, White Oak, Md.
(NOL technical report 61-67)
THE CHARACTERISTICS OF ELECTRIC SPARK DISCHARGES IN MIXTURES OF HIGH-EXPLOSIVE AND ALUMINUM POWDERS (U), by T.P. Liddiard, jr. 25 Aug. 1961. 36p. charts, diagrs. Task NOL-260. Project LACE. UNCLASSIFIED

A method is described for obtaining the average resistance of a spark discharging through a granular conductive mix in a non-oscillating discharge system. The spark resistance is a linear function of the spark gap width for a given electrode arrangement. The resistance is relatively independent of the density of the mix over the range 0.7 to 0.9 ohm.

Abstract card is unclassified

1. Explosives - Initiation
2. Explosives - Detonation
3. Explosive, High
4. RDX/aluminum
5. Sugar/aluminu
I. Title
II. Liddiard, Thomas P.
III. Project
IV. Project

Naval Ordnance Laboratory, White Oak, Md.
(NOL technical report 61-67)
THE CHARACTERISTICS OF ELECTRIC SPARK DISCHARGES IN MIXTURES OF HIGH-EXPLOSIVE AND ALUMINUM POWDERS (U), by T.P. Liddiard, jr. 25 Aug. 1961. 36p. charts, diagrs. Task NOL-260. Project LACE. UNCLASSIFIED

A method is described for obtaining the average resistance of a spark discharging through a granular conductive mix in a non-oscillating discharge system. The spark resistance is a linear function of the spark gap width for a given electrode arrangement. The resistance is relatively independent of the density of the mix over the range 0.7 to 0.9 ohm.

Abstract card is unclassified

1. Explosives - Initiation
2. Explosives - Detonation
3. Explosive, High
4. RDX/aluminum
5. Sugar/aluminu
I. Title
II. Liddiard, Thomas P.
III. Project
IV. Project